JAAS
Journal of Analytical Atomic Spectrometry

Accepted Manuscript

This article can be cited before page numbers have been issued, to do this please use: J. Touriniemi, T. R. Holbrook, G. Cornelis, M. Schmitt, H. Staerk and S. Wagner, *J. Anal. At. Spectrom.*, 2020, DOI: 10.1039/D0JA00243G.

ROYAL SOCIETY OF CHEMISTRY

rsc.li/jaas

View Article Online
DOI: 10.1039/D0JA00243G

ARTICLE

Measurement of number concentrations and sizes of Au nanoparticles spiked into soil by laser ablation single particle ICPMS

Received 00th January 20xx,
Accepted 00th January 20xx

DOI: 10.1039/x0xx00000x

Jani Tuoriniemi[a], Timothy R Holbrook[b], Geert Cornelis[a], Melanie Schmitt[c], Hans-Joachim Stärk[b], Stephan Wagner[b,*]

A novel method to directly quantify nanoparticles (NPs) in a soil matrix by laser ablation single particle inductively coupled plasma mass spectrometry (LA-sp-ICPMS) was developed. Different concentrations of 60, 100, or 250 nm diameter gold NPs (AuNP) were deposited directly on polyether sulfone (PES) ultrafiltration membranes or immersed in soil. The ICPMS sensitivity was calibrated using aqueous dissolved Au standards and an aqueous AuNP size standard dispersion was used to calculate the transmission efficiency. In case of the soil samples, sizing proved to be more accurate when calibration occurred while ablating a non-spiked soil. A linear relation was found between the spiked AuNP number concentrations and the particle event frequencies measured in the ablated area. Particle recovery on PES filters ranged only between 29 to 42 % and recovery of soil-spiked AuNP on thin tape was between 15 and 60 % and increased with size. However, 70-85 % mass recovery in the ablated area was obtained when the soil sample was deposited on a thicker, opaque double sided tape suggesting that the substrate material is instrumental in absorbing excess laser energy thus enhancing recovery. The rate of soil ablation and mass transfer into the plasma was quantified to calculate the recovery using the same soils spiked with indium. The presented method thus has a significant potential to be used for routine quantification of the particle size distributions of engineered or natural NPs in soil and possibly other powder samples with significantly fewer artifacts than extraction followed by aqueous analysis.

[a]Dept. Soil and Environment, Swedish University of Agricultural sciences (SLU), Lennart Hjelms väg 9, 75651 Uppsala.

[b]Helmholtz-Centre for Environmental Research. Dept. Analytical Chemistry, Permoserstraße 15, 04318 Leipzig

[c]Dept. Geosciences, Swedish Museum of Natural History, Box 50 007, SE-104 05 Stockholm, Sweden.

* corresponding author Stephan.wagner@ufz.de
Electronic Supplementary Information (ESI) available: ……

View Article Online
DOI: 10.1039/D0JA00243G

Introduction

The rapidly increasing use of nanoparticles (NPs) in industrial products has created a demand for legislation and environmental monitoring similar to conventional chemicals. Such monitoring programs would require measurement of number based particle size distribution (PSD) in complex matrixes given that many of the emerging regulatory definitions of a nanomaterial stipulate that a certain fraction of the particles by number must have one, or all dimensions below a threshold (*e.g.* 100 nm)[1]. Electron microscopy is not always a suitable base for such measurements, and therefore alternative methods have been explored.[2] Among these, nanoparticle tracking analysis (NTA) and single particle inductively coupled plasma mass spectrometry (sp-ICPMS) stand out in practicality[3] and via interlaboratory comparisons[4-9] are becoming accepted as standard methods for routine analysis. NTA can measure the number based PSD for those aquatic dispersions that are concentrated enough (>10^6 mL^{-1}) to allow observation of a statistically significant number of particles during a few minutes of analysis.[10] Trace level number concentrations (>10^2 mL^{-1}) can be characterized in dispersion by sp-ICPMS that quantifies the ion bursts coming from individual particles entering the plasma.[11] However, analysis is difficult for concentrated suspensions that might scatter light too strongly for NTA and be barely amenable for introduction into a plasma with a conventional nebulizer-spray chamber system.

The applicability of slurry nebulization for sp-ICPMS is limited. The deposition of solids rapidly blocked the ICP cones when nebulizing silver NPs (AgNP) spiked wastewater liquor containing 1-2 % organic particulate material, and a large fraction of the AgNP that were bound to particles larger than a few microns were lost in the spray chamber.[12] Efforts have therefore been directed at producing extraction or digestion protocols sparing the analyte particles. It is aimed to quantitatively transfer the particles from demanding matrixes such as biological tissues[13-16], food[17] or soil[18] into an aquatic dispersion suitable for conventional sp-ICPMS analysis. These procedures are, however, laborious and each new sample type could require a precarious attempt of method development. Rather, the ideal method should be able to characterize the sample in the most pristine state possible.

Up to now, it was possible to measure the number concentration (c_p) and equivalent spherical size (d_{part}) of gold NPs (AuNP) and AgNP dispersed in soil without any alteration of the sample with environmental scanning electron microscopy (SEM) using backscattered electron imaging (BSE) for counting the number of particles visible in a given area.[19] The unknown probing depth of the electron beam is, however, required for calculating c_p, because the sample volume where particles can be visualized must be known. In addition, the accuracy of sizing using SEM-BSE is reduced because the localization of the particle edges becomes less precise as the electron beam expands while it propagates in the sample. Furthermore, the analysis of environmentally relevant concentrations would require that an automated microscope would be run overnight probing a large sample area.

Particles embedded in a matrix can also be characterized by measuring the refractive index (n) of the sample.[20] The n of a composite material consisting of particles embedded in a solid or liquid matrix as a function of the c_p and d_{part} is given by the coherent scattering theory.[21] Fitting such theory to measured n values of a concentration series was used for determining these parameters for 100, 300, and 460 nm polystyrene latex dispersions within a few percent uncertainty. In a subsequent study[22] the method was used for determining the increase in vesicle concentrations inside the outer membrane of PC12 cells upon K^+ induced exocytosis. Any characterization based on measurement of n is, however, restricted to mass fractions larger than 0.1 % in transparent samples excluding soils.

Particle analysis has previously been investigated by surface assisted laser desorption (SALD) ICPMS where certain numbers of AuNP were deposited on a polymer sheet by evaporating a droplet of known volume and concentration of AuNP.[23] The AuNP were transferred mostly intact into a mass spectrometer within the optimal range of a set repetition rate and energy of the laser. Quantification of their number was possible once the transport efficiency (f_{trp}) from the polymer sheet into the ICP was determined. The f_{trp} is analogous to the nebulization efficiency (f_{neb}) that in liquid sp-ICPMS states the fraction of particles passing through the spray-chamber.[24-25] The equivalent spherical size can be calculated from signal intensities if the transmission efficiency (f_{trm}) of analyte from the plasma to the detector is also known.[24-25] f_{trm} is generally obtained by dividing the instrument sensitivity obtained during calibration by f_{trp}. Recently it has been demonstrated that this approach is also applicable to more complex samples. AuNP can be transferred intact from inside onion[26] and mouse liver cells[27] into the ICPMS.

The current study further develops this approach for powder samples such as soils. The idea is that by loosely applying the soil powder on a substrate, the soil can be quantitatively transferred to the ICPMS by ablating this substrate. The hypothesis was that the NPs would remain intact, similarly to the named studies, and the number-based equivalent spherical size distribution (PSD) could thus be obtained provided that f_{trp} could be quantified. Calibration for f_{trm} would preferably occur similarly to aqueous sp-ICPMS, *i.e,* using commonly available dissolved standards and one particle standard having a certified size.[28] Having a quantitative LA-spICPMS method available can be considered a substantial progress because it enables analysis of nanoparticles in complex matrices like soils without lengthy and error-prone sample preparation.

The AuNP in this work were first deposited on a flat ultrafiltration membrane surface to determine effects of particle concentration and laser energy on particle recovery (number & mass) as well as on the d_{part}. Thereafter ablation was investigated on AuNP spiked soil deposited on double sided tape. Calibration strategies were devised taking into account ionic suppression from the ablated soil, and the capabilities of measuring d_{part} of single and aggregated particles were assessed. The particle size-dependence of f_{trp} from the soil to the mass spectrometer was investigated. Two different strategies for measuring the c_p were explored: Particles were quantified by weighing the sample deposited on a tape with a known area, and assuming they are quantitatively transferred into the plasma from a given ablated area. Another strategy tested was calibrating for the rate of soil ablation by measuring indium spiked into the soil to a known concentration. Finally AuNP containing soil column fractions were analyzed as a demonstration of applicability.

View Article Online
DOI: 10.1039/D0JA00243G

Experimental

Instrumentation

Settings used when nothing else is stated of the two different ICPMS and LA-systems used in this work are given in Table 1. An iCAP Q ICPMS (Thermo Scientific) was used for the experiments with AuNP deposited from a droplet on a polyether sulfone (PES) ultrafiltration membrane and for investigating the size dependence of AuNP mass transfer from soil deposited on thin double sided tape. A high resolution (HR) sector field instrument (Attom, Nu instruments) capable of rapid (0.04 ms dwell time) acquisition was then used for more detailed investigation of the appearance of particle events and background signals, and to carry out the measurements of the soil column samples deposited on the optimal opaque tape substrate that effectively absorbed the laser energy. The Attom LA-ICPMS analyses were carried out at the Vegacenter at the Swedish Museum of Natural History. Using these two instrument configurations allowed to probe the capabilities of LA-spICPMS over a wide range of particle sizes where the high sensitivity of the HR-ICPMS system is more adapted to relatively small sizes, whereas larger particles can be measured by the quadrupole system without saturating the detector.

Table 1 LA-ICPMS instrumentation and settings

ICPMS instrument	Nu instruments Attom HR	Thermo iCAP Q
Spray chamber	Cyclonic Quartz	Cyclonic Quartz
Nebuliser	Micro-Mist glass	Thermo MicroFlow PFA-ST 1317090
Cool gas flow rate (L min^{-1})	13	14
Auxiliary gas flow rate (L min^{-1})	0.75	0.8
RF power (W)	1300	1550
Dwell time (ms)	0.04	3
Ablated area per sample (μm^2)	2-4*10^6 raster pattern	2-4*10^6 raster pattern
Dissolved standard concentrations (µg/L)	0.02,0.05, 0.1, 0.5	0.25, 0.5, 1, 5, 10
LA-System	ESI NWR 193 nm ArF	Analyte G2 193 nm ArF (Teledyne CETAC)
Laser spot dimensions (µm)	100 x 100	100 x 100
Laser spot shape	Rectangular	Rectangular
Feed gas flow rate (L min^{-1})	0.8	0.8
Laser energy (J cm^{-2}))	Max. 7.0	Max. 2.57
Scan speed (µm s^{-1})	100	100
Pulse frequency (s^{-1})	10	10
Particle sizes measured (nm)	10, 20, 40, 60	60, 100, 250

Particles and chemicals

Monodisperse, citrate-coated 20, 60, 80, 100, and 250 nm BBI AuNP (BBI, UK) were used. These NPs were characterized using aqueous sp-ICPMS and dynamic light scattering (DLS) immediately before spiking them into soil. Dissolved Au and In standards, cysteine and $CaCl_2$ were obtained from Sigma-Aldrich (USA). The Lufa 2.2 standard soil was used[29], a sandy loam soil that is recommended as a standard medium for NP testing.[30]

Particle deposition on polyethersulfone (PES) membrane filters

0.5 µL of 60 nm AuNP suspension and 1 µL of 100 nm AuNP suspension was applied by drop deposition onto a 30 kDa PES membrane (Millipore, Burlington, USA). The final particle mass concentration ranged between 7.1 and 56.8 µg L^{-1}. After air drying, each spot was completely ablated and each experiment was performed as a triplicate.

Soil spiking

The spiking of AuNP into Lufa 2.2 soil was done in two different ways. A first method consisted of simply adding and mixing in NP suspension with soil as in an earlier SEM study[19]. Briefly, 100 µL AuNP suspension was diluted to different concentrations using ultrapure water and this suspension was added to ca. 0.5 g of soil in 5 different 20 µL aliquots followed by vigorous manual mixing to spread each droplet evenly in the soil before adding the next one. The number concentrations in soil were in the range ~7.1x10^9-1.5x10^8 g^{-1} for the 60 nm particles, an order of magnitude lower for the 100 nm AuNP, and within ~4x10^7-7.9x10^5 g^{-1} for the 250 nm ones. In the second method, saturated column experiments were done as outlined in Norrfors *et al*.[31] Shortly, two pore volumes of diluted suspensions of the 20 or 80 nm AuNP were injected, bottom up, in repacked, saturated columns of Lufa 2.2 soil using a flow rate of 0.4 mL min^{-1}.

For determination of total elemental concentration the spiked soils were air-dried and digested using *aqua regia* in a microwave using a standard protocol.[32] The digests were diluted using 3 vol% HCl prior to ICPMS analysis.

To investigate whether aggregates are measured intact during LA-spICPMS, 60 nm AuNP were aggregated by adding 1 mM $CaCl_2$ to the NP suspension. After 15 min an aliquot was spiked into the soil using the first method, while a second aliquot was promptly diluted 10^5 times using 1 mM $CaCl_2$ and measured in dispersion with spICPMS calibrated using dissolved Au standards diluted using 1 mM $CaCl_2$. In-spiked soil was created to investigate the ablation rate of soils. Dry soil was immersed in a 0.5 ppm In solution for 24 hours followed by filtering using 0.2 □m centrifugal filter tubes (Sartorius, Germany) followed by air-drying at 50°C overnight.

Soil sample preparation.

Dried spiked (with AuNP or In) soil was additionally homogenized in an agate mortar before spreading it evenly on a piece of thin plastic double sided tape (tesa® Double-Sided Tape Universal, thickness approx. 0.2 mm) having a known weight and area, in case of the quadrupole experiments or a thicker, double sided tape (tesa® Powerbond mounting tape, approx. 2 mm thickness) in the case of the HR-ICPMS experiments The structure of the latter tape was a two millimeter thick foam cushion. Excess soil not sticking to the tape was removed using a nitrogen gas stream and the tape piece was weighed again in order to know the average attached mass of soil per unit area. The tape piece was subsequently attached to a glass slide that was mounted into the ablation cell.

View Article Online
DOI: 10.1039/D0JA00243G
ARTICLE Journal Name

Transmission efficiency (f_{trm}) determination and measurement.

Calibration and f_{trm} determination of the quadrupole ICPMS for measurements on the PES surfaces was done using a T-section with one of the inlets connected to a nebulizer spray-chamber system and the second one to the ablation cell (Figure 1). Dissolved Au and particle standards were diluted in 0.1 mass-% cysteine solutions to avoid carry-over[33]. The standards were injected via the nebulizer while ablating empty PES sheets to correct for the ionization suppression effects brought by the ablation fragments. The f_{trm} was calibrated according to the method of Pace *et* al.[28] using the 60 nm AuNP suspensions. Upon ablating the samples a cysteine blank was nebulized to preserve the plasma conditions upon calibration.

When the quadrupole instrument was calibrated for measuring the soil samples, the plasma was connected either to the spray chamber, or the ablation cell. No correction for ionic suppression was thus made for this set of samples.

The HR instrument plasma torch was also coupled via a T-section to both the LA-system and a desolvator (DSN-100 system/Aridus II) (Figure 1a). Dissolved Au and particle standards (40 and 60 nm) were in a similar way diluted in 0.1 mass-% cysteine solutions and were injected via the desolvator while ablating a non-spiked soil sample (Figure 1b) to matrix-match ionization suppression due to the flux of ablation fragments into the plasma while measuring spiked samples. A 0.1 % cysteine solution was injected again while measuring the AuNP spiked soil samples to keep plasma conditions as close as possible to what they were during calibration (Figure 1b).

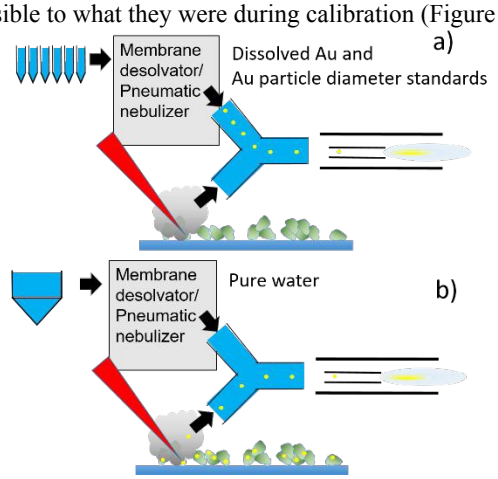

Fig. 1 A schematic showing the experimental setup for a) calibration and b) measurement with the mass spectrometers. Membrane desolvator unit was used in combination with Nu instruments Attom HR instrument. The pneumatic nebulizer unit was used in combination with the iCAP Q Thermo instrument.

Data treatment.

The particle peaks measured with the HR-ICPMS were detected and quantified using an improved algorithm based on Tuoriniemi *et al.*[34]. The new data analysis program among other things reduces the risk of noise causing a single particle event to appear as several events. A thorough description of the new algorithm and discussion about particle detection will be published elsewhere. The most important parameter set was the iterative 6σ criterion for detecting the particles as outliers. The average signal not considered to be a part of any particle event was subtracted from the particle signals to correct for the background. Equivalent spherical sizes were calculated from the signal intensity of discriminated particle events using the f_{trm}.

The quadrupole signals were quantified using methods[25] for conventional non-FAST ICP-MS. An iteratively set 6σ criterion was again chosen as a detection threshold. Calculation of particle and mass recovery as well as equivalent spherical size are detailed in the result section.

Results and discussion

Desorption from PES filter surfaces

Particle size preservation and linear concentration response. The equivalent spherical size and linearity of a concentration series of the 60 and 100 nm AuNP were examined with the quadrupole ICPMS system coupled to an LA system using a laser energy of 0.48 J/cm^2 (Figure 2, Figures S.1, S.2, and S.3). nm^{-1} as units for particle frequency indicates that the frequencies are normalized to the bin size to give equal weight to each bin. The modal equivalent spherical diameter was within 8% of the nominal modal diameter as characterized using transmission electron microscopy for both 60 and 100 nm NPs. A second population of small particles (< 40 nm) appeared for the 60 nm AuNP that was not present in the dispersion. It partly consists of fragmented NPs and/or dissolved Au in the dispersions that precipitated as < 40 nm particles upon drying. While high in number, the mass fraction of these small particles was below 10 %.

The linearity of the detector response in terms of mass and number concentration in the deposited dispersions was measured at four different mass concentrations between 7.1 and 56.8 µg L^{-1}. These experiments demonstrated good linearity for both 60 and 100 nm Au NPs with R^2 values between 0.92 and 0.99 for mass and particle number concentration (Figure S.1).

Recovery

The recovery (R) is determined as the product between the f_{trp} and the mass fraction of particles/analyte that is effectively ablated or desorbed (f_a):

$$R = f_a f_{trp} \quad (1)$$

Benesova *et al.*[23] implicitly assumed $R = f_{trp}$, *i.e.* these authors did not distinguish between processes occurring during the ablation stage that determine f_a and processes that reduce the analyte and/or particle concentration in the aerosol travelling from sample to ICP. Because it was not possible to distinguish between the ablation (f_a) and the transport efficiency (f_{trp}) in this set of experiments we also report total recovery values without distinguishing between f_a and f_{trp}.

When the AuNP were deposited onto a PES membrane surface, and the entire area with AuNP deposits was desorbed by a relatively weak laser beam the total mass R were 34 and 54% and intact particle mass R 29% and 42% for 100 and 60 nm AuNP respectively (Figure 2 a, b, Table S.1). Using laser energies higher than 0.48 J/cm^2 resulted in even lower R (Table S.1). In repeated ablations of the same areas, no more than 2% of the total deposited AuNP mass was determined. The loss of AuNP may instead be explained by a spread and loss of NP in the ablation cell during the ablation process. Factors influencing

View Article Online
DOI: 10.1039/D0JA00243G

the f_{trp} are discussed further below. The determined mass *R* were comparable to the previous study of Benesova *et al.* who obtained 61% for 56 nm AuNP deposited on PETG sheets.[23] The same study also reported that the measured equivalent spherical size was not altered by LA-spICPMS analysis.

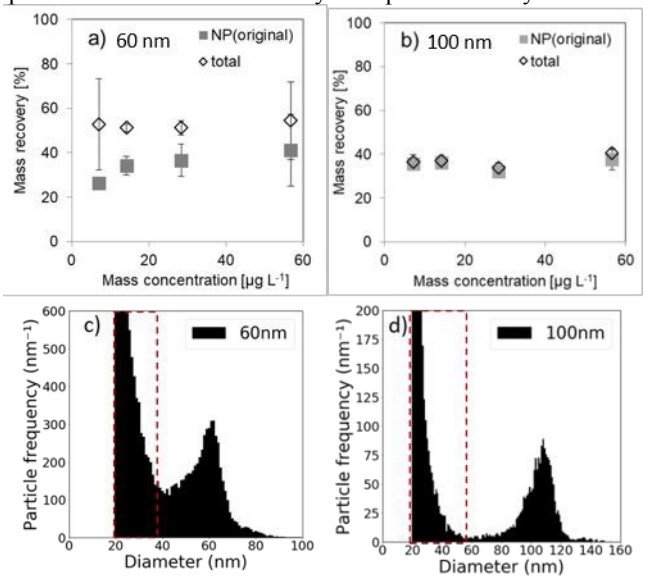

Fig. 2 a-b) Total mass recovery and particle number recovery for 60 nm and 100 nm AuNP deposited om a PES membrane in a mass concentration range between 7.1 and 56.8 µg L^{-1} as well as c-d) AuNP particle size distributions for nominally 60 nm (56.6 µg L^{-1}) and 100 nm (56.8 µg L^{-1}) determined with LA-spICPMS (laser energy 0.48 J cm^{-2}), n=3, Note that the PSD was calculated from data where background events were subtracted iteratively using a 6σ-criterion. The dashed red line boxes indicate the possibly fragmented particles.

Soil Ablation

Equivalent spherical size distributions of monomers. The PSDs of 60, 100, and 250 nm nominal diameter BBI AuNP dispersed in soil (8.86, 11.4, 32.4 µg g^{-1}) deposited on thin tape were measured at a laser energy of 0.48 J cm^{-2} using a quadrupole ICPMS instrument having dwell times in the ms range (Figure 3). For each of the tested particles sizes, a peak can be seen having a median equivalent spherical diameter close to its nominal value and a second peak consisting of numerous relatively small particles. Similar PSDs were also obtained for AuNP at the PES surfaces (Figure 2). The larger peaks contain most of the AuNP mass (> 98 %) and closely match the PSDs that were spiked into the soil despite of the lack of correction for ionic suppression effects. The AuNP are therefore mostly transferred intact from the soil into the ICPMS. The smaller peak probably mostly consists of fragments, because the maximal size of this fraction increases with the spiked AuNP diameter. Besides fragmented AuNP, a part of the small particle events could be dissolved Au adsorbed to the soil fragments. Soils typically have a natural Au background of a few µg Kg^{-1}, and the < 1% dissolved Au in the particle dispersions could have added up to a few tens of µg Kg^{-1} dissolved Au. These ions are assigned to small particle events even when using a conservative detection threshold, because this background concentration does not form any continuous dissolved signal as it would do during aqueous spICPMS. Their abundance will determine the smallest measurable size in a way analogous to the dissolved signal noise levels in liquid spICPMS. The mass fraction of Au not included in any particle events by the algorithm was < 1% for all soil samples measured. Note that the washout time of the ablation chamber was long enough for there to be no periodicity in particle arrivals or background signal corresponding to the 10 Hz ablation rate.

The results in Figure 3 show that accurate sizing is possible up to at least ca. 250 nm, where signal clipping starts to affect results when using a quadrupole ICPMS. It has been found that ablation fragments from soil are mostly > 1 µm in diameter[35] and they could allow the considerably smaller AuNP to remain intact embedded or adsorbed on their surfaces.

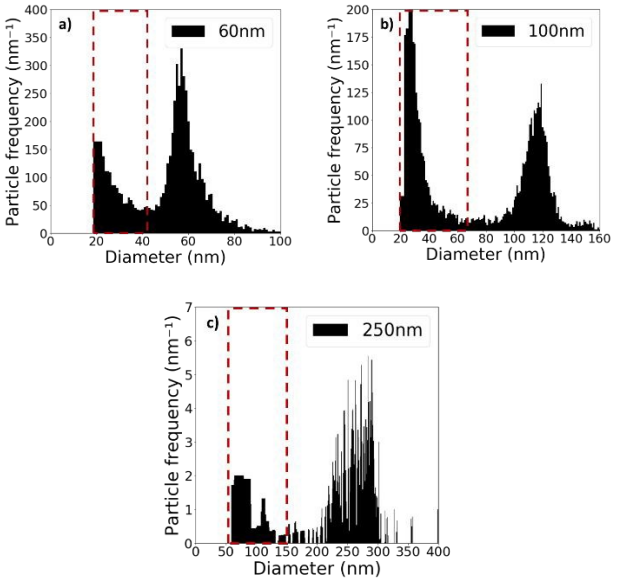

Fig. 3 Size distributions of a) 60, b) 100, and c) 250 nm AuNP dispersed in soil. The dashed red line boxes indicate the spurious background particle events. Note that the PSD was calculated from data where background events were subtracted iteratively using a 6 σ - criterion.

PSD of aggregated particles

The Au mass-based PSD of the previously aggregated 60 nm AuNP that were spiked in soil and measured using LA-spICPMS are compared with the PSD measured in 1 mM $CaCl_2$ suspensions using aqueous spICPMS in Figure 4. The majority of the particles are aggregates in the aqueous suspensions having an equivalent spherical diameter larger than 100 nm. The LA-spICPMS sample of soils spiked with these aggregates, however, show that the average aggregate equivalent spherical size decreases upon ablation. Most of the aggregates apparently were broken up during the ablation process even though primary particles are left intact by LA-sp-ICPMS.

View Article Online
DOI: 10.1039/D0JA00243G
ARTICLE Journal Name

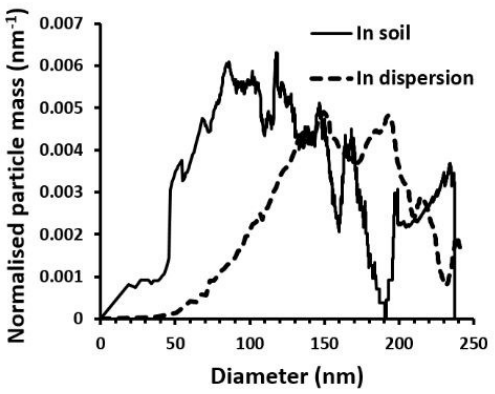

Fig. 4 Au mass based PSD of 60 nm BBI particles aggregated by addition $CaCl_2$ in aqueous dispersion and spiked into soil.

Linearity of concentration response

Both the number of particles and the total detected Au mass detected in a given ablated area of spiked Lufa 2.2 soil were linearly dependent on the spiked concentration (Figure S4). The duration of a scan was 40 seconds during which time, 4000 µm^2 of soil-covered surface was ablated. The result for each sample is an average of at least 9 replicate scans from the same tape in an effort to reduce statistical noise on the average. The dynamic range in terms of number concentration was similar to that of aqueous spICPMS, *i.e.* at least 3 orders of magnitude[25]. The R^2 values for fitted lines were > 0.99 for the number concentrations of the 250, 100, and 60 nm AuNP, and 0.99, 0.98 and 0.99 respectively for the corresponding mass concentrations.

Size dependence of recovery

Quantification of the number concentration of unknown samples requires the R to be known. The entire spiked area could not be ablated as opposed to experiments with PES surfaces ablated. R therefore has to be calculated differently. A known mass of soil (W_s) containing a known AuNP number (c_p) and mass concentration (c_s) was typically deposited as a 10-15 µm thick layer on a piece of tape having a known surface area A_t. An estimate of the R of NPs from a soil with known AuNP concentration during LA-spICPMS can thus be calculated when one knows the ablated area (A_s). The total particle number or mass of analyte reaching the plasma (M_m) while ablating the area (A_s) relates to c_s as:

$$M_m = \frac{f_a f_{trp} A_s c_s W_s}{A_t} \quad (2)$$

Combining eqs. (1) and (2), the recovery of particles number or mass in the ablated area is thus defined as:

$$R = \frac{M_m A_t}{A_s c_s W_s} \quad (3)$$

The values for R shown in Figure 5 were calculated for the two highest spiked Au concentrations of each size, because the relative importance of spurious background particle contamination is smaller for these samples (see Figure S4). The mass and number based R are shown as a function of nominal size. They increased non-linearly when the nominal size increases from 60 nm to 250 nm. The R values for number concentrations ranged from ~ 15 to ~ 60 % indicating that most of the particles were not transferred from the tape into the plasma. There was a close match between the number and mass based values, because the mass of smaller particles, which were not included in the particle number count, was negligible relative to the larger particles for all samples. Particle fragmentation can thus not explain the low recovery. These results confirm the low recoveries observed during the samples on PES surfaces where we observed also a loss attributable to a spread and loss in the ablation cell, but no strong size dependence.

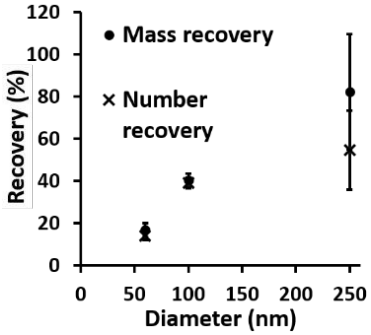

Fig. 5 Number and mass based recoveries of AuNP (60, 100, 250 nm). The values are calculated from the two highest spiked concentrations for each nominal size.

f_{trp} has previously been found to depend on the size of ablation fragments, but only if these fragments were relatively large. f_{trp} was more than 80% for ablation of molybdenum metal fragments between 5 nm to 2 µm, small particles being lost because of diffusion and the larger ones because of settling.[35] The f_{trp} of volatile metals such as In was 64%, while it was 20% or lower for Al, Cu, Ni, Sb, Sn, as the size of particles produced were larger.[36] Garcia *et al.*[37] showed that the f_{trp} was at least 75% regardless of the type of ablation cell used when brass was ablated with a femtosecond laser producing aerosols in the size range 5 nm - 1 µm.

Two different explanations can be found for the observed low size-dependent recoveries of AuNP. The overall low R indicates that the NPs likely remained attached to large soil particles that do not detach or settle in the ablation cell. Secondly, the diffusion coefficient of small particles is higher and thus also the probability that these collide with and attach to the ablation cell and/or connection tubes leading to the ICP. The second explanation is, however, unlikely, because no size dependence of recovery was observed between the 60 and 100 nm particles

View Article Online
DOI: 10.1039/D0JA00243G

in the experiments with PES surfaces. Small NPs are therefore more likely to be strongly bound to soil particles compared to larger NPs and small NPs are thus removed proportionally more together with these large soil particles.

Quantitative soil ablation and trace particle analysis with LA-HR-ICPMS.

A size-dependent, low recovery obstructs quantification of number concentrations by LA-spICPMS of unknown samples. Other substrates where the ablation is more efficient were therefore investigated. Absorption of laser energy in the underlying substrate is likely to play a role because the soil layer itself is relatively thin. A thicker, opaque tape with a porous surface that possibly more efficiently absorbs the laser energy was therefore tested using the second ICP-MS system in Table 1.

Figure 6 a) shows the calibration curves that were measured with or without simultaneous ablation of soil. The f_{trm} in the presence of soil was reduced by a factor of 0.71 due to ionic suppression. Figure 6 b) shows the PSD of the same AuNP suspension, but calculated with and without taking the effect of ablation into account during calibration and f_{trans} determination. It can be theoretically calculated that the equivalent spherical size would be underestimated with a factor of 1/3 if the f_{trm} not corrected for ionic suppression is used for calculating the unknown equivalent spherical diameter. The bias due to ionic suppression was smaller in the previous quadrupole experiments because the water was not removed with a membrane desolvator upon calibration, and the sensitivity decrease brought by the droplets happened to match the suppression by the soil when the plasma was connected to the ablation cell instead.

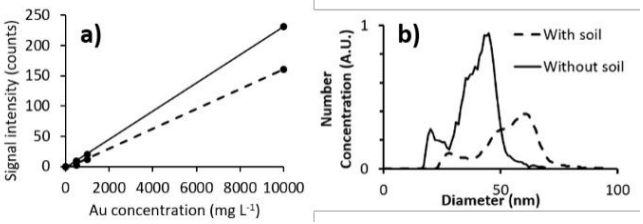

Fig. 6 Comparison of the effect of simultaneously ablating soil ("with soil") or not ("without soils") on a) the calibration curves obtained from dissolved Au standards and b) the PSD of an aqueous AuNP suspension having a nominal size of 60 nm.

The rapid data acquisition with a 0.04 ms dwell time allowed the AuNP particles events from soil to be studied in detail (Figure S5a). They are similar to AuNP events from liquid dispersions (average FWHM = 0.12 ms).

The In concentration retained in the spiked soil was determined to 46 ppb using the *aqua regia* digestion method described above. The signal upon ablation from tape (Figure S5b) further illustrates that not even a dispersed ionic analyte forms a continuous background signal known to occur in the case of spICPMS of aqueous ionic solutions. This implies that outlier-based particle event detection is less effective in the case of LA-spICPMS, because this approach assumes that non-particle events occur as a continuous background.

Effect of laser energy on recovery and ablation rate

The values of number-based R measured for soil deposited on the opaque foam tape are shown in Figure 7 as function of laser energy. At all tested energies, the CCD camera observations made by the LA system during ablation suggested that the laser beam cleared the soil from the adhesive tape within the path of the laser beam. However, some of the soil alongside the laser beam path was possibly also removed during LA scans. Tests where the beam repeatedly traversed the same path with these settings showed that > 80% of the analyte that was to reach the plasma did so during the first run (Figure S6). As for the PES substrate, the R during LA-sp-ICPMS can thus not be improved by increasing the beam exposure using a slower scan speed or by a faster pulse frequency, but instead, NPs outside the laser beam path could have been taken up leading to a higher apparent R. Figure 7 shows how R increases as a function of laser energy from ~ 60 % at the lowest (0.5 J cm^{-2}) and highest value tested (7 J cm^{-2}) to ~ 80 % at the optimum value of 3 J cm^{-2} of laser output. These differences were, however, barely significant as the 95% confidence intervals due to fluctuations between 2-4 repeated 40 s line scans overlap. With a more suitable substrate it is thus possible to reach an R close to 1. Note that around an order of magnitude higher laser energies were required to ablate soil from the tape surfaces than for the AuNP directly deposited on the PES membrane.

The source of the variance between scans was not due to an insufficiently high counts, but rather because of the heterogeneity in AuNP concentration on the tape surface. In a LA-sp-ICPMS experiment, this variance component is typically eliminated by ablating the whole adsorbed droplet as it was done with AuNP deposited onto the PES membrane. Complete ablation of a 1-2 cm^2 tape is, however, not realistic nor is it practically possible to concentrate soil homogeneously in a small enough point to be ablated completely. The 95 % confidence interval in Figure 7 on c_p Δ due to concentration variations can be estimated from:

$$\Delta_{95\,\%M_m} = 1.96N^{-0.5}(1-f_m)^{0.5}\sigma_{cp} \qquad (4)$$

Where N is the number of scans measured, the f_m is the fraction of sample surface measured in the whole set of scans, and σ_{cp} is the standard deviation in local measured particle frequency varying between subsequent scans. The locations of the scans are assumed to be representative for the sample in the sense that an accurate enough estimate for σ_{cp} was obtained. The RSD among scans each 40 s in duration was 20% for AuNP and 31% for In while only a negligible fraction of the whole tape surface was ablated. This is comparable to the percentage of analyte lost during transfer from the tape surface and in most cases therefore does not significantly add additional uncertainty to the analysis.

View Article Online
DOI: 10.1039/D0JA00243G
ARTICLE Journal Name

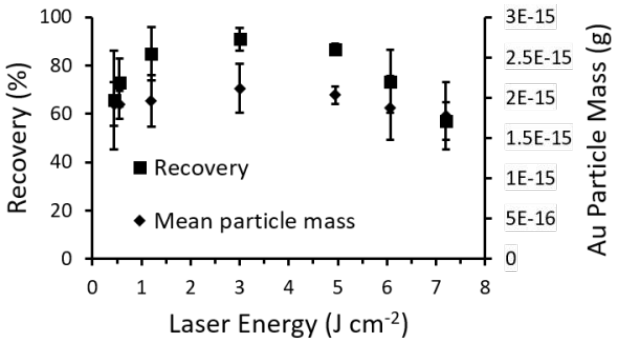

Fig. 7 Effect of laser energy on the measured average particle mass and recovery of number concentration. The error bars are the 95 % confidence interval of the mean among replicate measurements.

Bias is introduced to the concentration calculated from eq. 3 unless close to 100 % recovery is reliably achieved. Additional error could be introduced by any inaccuracy in the weighing of mg quantities of soils and that the ablated area is not clearly defined. It can therefore be advantageous to use the ablation rate ($r_{ablation}$) of soil delivered into the plasma during a time of measurement (t_m) determined by using a sample component of known concentration as a proxy. We therefore added In to the soil to more accurately calculate $r_{ablation}$.

$$r_{ablation}=M_m c_s^{-1} t_m^{-1} \quad (5)$$

The In-based $r_{ablation}$ is shown in Figure 8 for several laser energies.

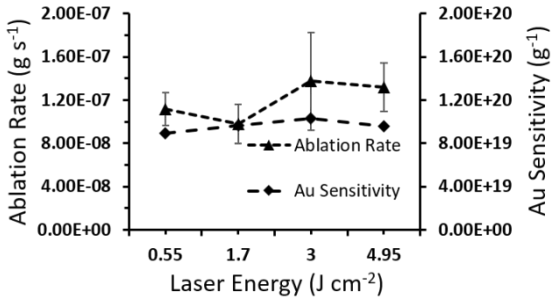

Fig. 8 The $r_{ablation}$ for deposited Lufa soil determined by the known concentration of spiked indium, and the sensitivity f_{trm} of dissolved Au in terms counts per mass of dissolved Au entering the plasma determined while ablating the soil with the given laser energy.

The In and Au sensitivity ($f_{neb}f_{trm}$) was calibrated separately for each laser energy. The differences in $r_{ablation}$ between the laser energies were minor. It was also confirmed that these differences were not caused by varying levels of ionic suppression because the up to 20 % differences in Au sensitivity in Figure 8 did not, or only weakly correlated with the $r_{ablation}$. The $r_{ablation}$ thus seems to be a parameter that is more stable between replicate samples than the R determined via weighing and $r_{ablation}$ could therefore be used instead to determine c_s and c_p, but only if elemental fractionation effects[38] are assumed equal between Au and In.

Analysis of AuNP in soil colums

In order to demonstrate the applicability of the new analytical method, number and mass concentrations were measured with the HR instrument for 20 and 80 nm AuNP retained on the topmost 0.5 cm on a soil column in a mobility experiment. The PSDs are shown in Figure 9. The particles have undergone only little alteration in the soil. The tail of larger particles for the 20 nm sample could indicate homoaggregation or accumulation on the same soil grain. The total Au concentrations in the 20 and 80 nm column samples were 4.7 ± 2.0 ppb and 7.1 ± 2.0 ppb respectively, using the $r_{ablation}$ with the uncertainty according to eq. 4 being the 95% confidence interval among at least 8 40 s line scans (~ $3.2*10^{-4}$ cm^2) measured with 1.7, 3, and 5 J cm^{-2} laser energies. The corresponding values determined by weighing the soil and assuming R is equal to 1 were 1.9±1.1 ppb and 3.3±2.9 ppb, respectively. The concentration values determined by weighing are slightly lower than the ones based on the $r_{ablation}$, probably because full recovery was not achieved. On the other hand, uncertainties of tens of percent are typical, even for c_p determination in the liquid state using aqueous sp-ICPMS.[3-8]

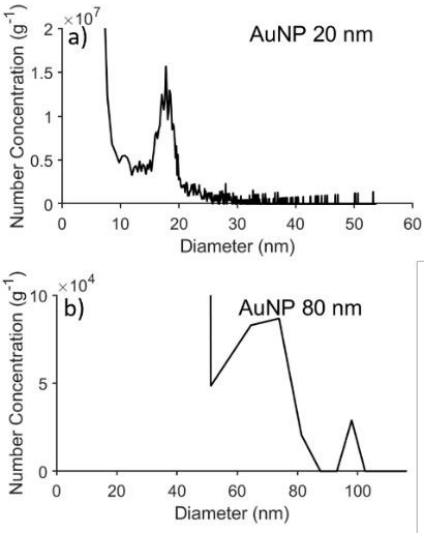

Fig. 9 PSD of a) 20 and b) 80 nm AuNP retained in soil columns.

Conclusions and outlook

It was demonstrated that the equivalent spherical size of particles can be quantified in soil following the same calibration procedures used for aqueous sp-ICPMS, i.e. using aqueous standards and size-certified particles. Sizing was only accurate, however, by matrix matching, i.e. simultaneously ablating a non-spiked soil. Determination of particle number concentration requires calculating the amount of soil that entered the plasma. Two methods were proposed: determination of the recovery by weighing the soil deposited before and after ablation and determination of the ablation rate using another element than the one of which the unknown NPs consist. Calibration using the ablation rate was found to be the most accurate approach because the results are less affected by an unknown and potentially low recovery. It was also found that high recoveries can be obtained using LA-spICPMS, but the choice of substrate has a significant impact on the recovery, an observation that warrants further research. LA-spICPMS thus

View Article Online
DOI: 10.1039/D0JA00243G
Journal Name ARTICLE

has a high potential for a total determination of NPs in soil and likely also other solid samples. The method scans a given volume of soil 10^3-10^4 times faster than SEM[19] which could render it an effective tool for environmental monitoring. It also enables direct analytical access to NPs without prior particle extraction. In future this initial exploratory study should be complemented with accuracy and reproducibility studies. It should be also explored if instrumental adaptation e.g. optimization of the LA sample chamber may improve NP recovery.

Conflicts of interest

There are no conflicts to declare.

Acknowledgements

The funding of the ACEnano project within the European Union Horizon 2020 Program (H2020, grant agreement number 720952) is greatly acknowledged. The authors appreciate the support of ProVIS Center for Chemical Microscopy by the Helmholtz Centre for Environmental Research – UFZ and the funds for ProVIS establishment provided by EFRE (Europäischer Fonds für regionale Entwicklung) and the federal state (Freistaat Sachsen). The Attom LA-ICP-MS analyses were carried out at the Vegacenter at the Swedish Museum of Natural History under Vegacenter contributions 049 and 063.

References

1. Boverhof D.R.; Bramante C.M.; Butala J.H.; Clancy S.F.; Lafranconi M.; Jay West J.; Steve C. Gordon, S.C. *Reg. Tox. Pfarm.* **2015**, *73*, 137-150.
2. Brown, S.C; Boyko, V; Meyers, G.; Voetz, M.; Wohlleben, W. *Env. Health Persp.* **2013**, *121*, 1282–1291.
3. Tuoriniemi. J, **2013** PhD Thesis University of Gothenburg.
4. Montoro Bustos, A.R.; Petersen, E. J.; Possolo, A.; Winchester, M.R. *Anal. Chem.* **2015**, *87*, 8809-8817.
5. Linsinger, T.P.J.; Peters, R.; Weigel, S. *Anal. Bioanal. Chem.* **2014**, *406*, 3835-3843.
6. Weigel, S.; Peters, R.; Loeschner, K.; Gromle, R.; Linsinger, T.P.J. *Anal. Bioanal. Chem.* **2017**, *409*, 4839-4848.
7. Proficiency test ACEnano for gold nanoparticles in water. RIKILT Waeningen, the Netherlands, RIKILT Report 2018.519.
8. Caterina Minelli, Vamas TWA34 Project 10, National physical laboratory, Presentation.
9. Hole, P., Sillence, K., Hannell, C. et al. *J. Nanopart. Res.* **2013**, *15*, 2101.
10. Gallego-Urrea, J.A.; Tuoriniemi, J.; Hassellöv, *Trac Trend. Anal. Chem.* **2011**, *30*, 473-483.
11. Montaño, M.D.; Olesik, J.W.; Barber, A.G.; Challis, K.; Ranville, J.F. *Anal. Bioanal. Chem.* **2016**, *408*, 5053–5074.
12. Tuoriniemi. J.; Jurgens, M.; Hassellöv, M.; Cornelis, G. *Environ. Sci.: Nano* **2017**, *4*, 1189-1197.
13. Loeschner,K.; Navratilova, J.; Kobler, C.; Molhave, K.;Wagner, S.; von der Kammer, F.; Larsen, E. H. *Anal. Bioanal. Chem.* **2013**, *405*, 8185-8195.
14. Loeschner,K.; Brabrand, M. S. J.; Sloth, J. J.; Larsen, E. H. *Anal. Bioanal. Chem*. **2014**, *406*, 3845-3851.
15. Gray, E.P.; Coleman, J.G.; Bednar, A.J.; Kennedy, A.J.; Ranville, J.F.; Higgins, C.P. *Env. Sci. Tech.* **2013**, *47*, 14315-14323.
16. Peters, R.J.B.; Rivera, Z. H.; van Bemmel, G.; Marvin, H. J. P.; Weigel, S.; Bouwmeester, H. *Anal. Bioanal. Chem.* **2014**, *406*, 3875-3885.
17. Loeschner, K.; Correia, M.; López Chaves, C.; Rokkjær, I. Sloth, J.J. *Food Additives & Contaminants: Part A*, **2018**, 35:1, 86-93
18. Schwertfeger, D. M.; Velicogna, J.R.; Jesmer, A. H.; Saatcioglu, S.; McShane, H.; Scroggins, R.P.; Princz J.I. *Anal. Chem.* **2017**, *89*, 2505−2513.
19. Tuoriniemi, J.; Gustafsson, S.; Olsson, E.; Hassellöv, M. *Env. Chem.* **2014**, *11*, 367-376.
20. Tuoriniemi, J.; Moreira, B.; Safina, G. *Langmuir* **2016**, *32*, 10632– 10640.
21. Barrera, R. G.; Garcia-Valenzuela, A. *J. Opt. Soc. Am. A* **2003**, *20*, 296-311.
22. Moreira, B.; Tuoriniemi, J.; Kouchak Pour, N.; Mihalčíková, L.; Safina, G. *Anal. Chem.* **2017**, *89*, 3069-3077.
23. Benešová, I.; Dlabková, K.; Zelenák, F.; Vaculovič, T.; Kanický, V.; Preisler, J. *Anal. Chem.*, **2016**, *88*, 2576–2582.
24. Laborda, F.; Jimenez-Lamana, J.; Bolea, E.; Castillo, J.R. *J. Anal. At. Spectrom.*, **2011**, ***26***, 1362-1371.
25. Tuoriniemi, J.; Cornelis, G.; Hassellöv, M. *Anal. Chem.* **2012**, *84*, 3965-3972.
26. Yamashita, S.; Yoshikuni Y.; Obayashi, H.; Suzuki, T.; Green, D.; Hirata, T. *Anal. Chem.*, **2019**, *91*, 4544–4551.
27. Li, Q; Wang, Z.; Mo, J.; Zhang, G.;Chen,Y.; Huang, C. *Sci. Rep.* **2017**, *7*, Article number: 2965.
28. Pace, H. E.; Rogers, N. J.; Jarolimek, C.; Coleman, V. A.; Higgins, C. P.; Ranville, J. F. *Anal. Chem*. **2011**, 83, 9361–9369.
29. Speyer, L. Standard Soils. http://www.lufa-speyer.de/index.php/dienstleistungen/standardboeden/8-dienstleistungen/artikel/57-standard-soils
30. Geitner, N.K.; Hendren, C.O.; Cornelis, G.; Kaegi, R.; Lead, J.E.; Lowry, G.; Lynch, I.; Nowack, B.; Petersen, E.; Bernhardt, E.; Brown, S.; Chan, W.; de Garidel-Thoron, C.; Hanson, J.; Harper, S.; Jones, K.; von der Kammer, F.; Kennedy, A.; Kidd, J.; Matson, C.; Metcalf, C.; Pedersen, J.; Peijnenburg, W.J.G.M.; Quik, J.T.K.; Rodrigues, S.M.; Rose, J.; Sayre, P.; Simonin, M.; Svendsen, C.; Tanguay, R.; Tufenkji, N.; van Teunenbroek, T.; Thies, G.; Tian, Y.; Rice, J.; Turner, A.; Liu, J.; Unrine, J.; Vance, M.; White, J.C.; Wiesner, M.R. **2020**. *Environ. Sci.: Nano*. *7*, 13-36.
31. Norfors, K.K.; Cornelis. G. 2019. *Accepted for publication in Environ. Sci.: Nano (*DOI: 10.1039/C9EN00448C).
32. Method 3051A: Microwave assissted acid digestion of sediments, sludges, soils, and oils, US Environmental protection agency, Washington D.C., 1998.
33. Chen, W. C.; Wee, P.; and Brindle, I. D. *J. Anal. At. Spectrom.* **2000**, *15*, 409–413.
34. Tuoriniemi, J.; Cornelis, G.; Hassellöv, M. ***J. Anal. At. Spectrom.*** **2015**, ***3 0***, 1723-1729.
35. Arroyo, L.; Trejos, T; Gardinali, P. R.; Almirall, J.R. *Spectrochim. Acta B* **2009**, 64, 16–25.
36. Arrowsmith, P.; Hughes, S.K. *Appl. Spectrosc.* **1988**, *42*, 1231-1239.
37. Huang,Y.; Shibata,Y.; Morita, M. *Anal. Chem.* **1993**, *65*, 2999-3003.
35. Garcia, G.G.; Lindner, H.; Niemax, K. *Spectrochim. Acta B* **2007**, *62*, 13–19.
38. Koch, J.; D. Günther, D. *Anal. Bioanal. Chem.* **2007**, *387*, 149–153.

View Article Online
DOI: 10.1039/D0JA00243G

ARTICLE